Isomerization and dehydrogenation of highly vibrationally excited azulene+ produced via S2 vibrational manifold

M.V. Vinitha, Arya Nair, Abhishek Kumar, Valérie Blanchet, Umesh Kadhane

Isomerization and dehydrogenation of highly vibrationally excited azulene$^+$ produced via S_2 vibrational manifold

M V Vinitha [a], Arya M Nair [b], Abhishek S Kumar [c], Valerie Blanchet [d], Umesh R Kadhane [a,*]

[a] Indian Institute of Space Science and Technology, Thiruvananthapuram 695547, Kerala, India

b Government College, Karyavattom, University of Kerala, Thiruvananthapuram 695581, Kerala, India

c Indian Institute of Science Education and Research, Thiruvananthapuram 695551, Kerala, India

d Universite de Bordeaux, CELIA-UMR5107 Domaine du Haut Carre, 43 rue Pierre Noailles, 33405 Talence Cedex, France

Abstract

High resolution energy-ToF correlation spectrometer and a nanosecond laser is employed to extract Hloss rate in hot azulene cations in UV region. Correlation between the photon wavelength and H-loss rate is obtained for 3-photon process and it is explained by a two-step mechanism: (i) 1+1 ionization with ultrafast internal conversion to the long-lived S_2 state (ii) the increase of internal energy by absorption of the third photon and isomerization. The work uncovers the role of S_2 state dynamics in Azulene in controlling the internal energy to a very narrow range.

INTRODUCTION

Azulene (az) and naphthalene (nph) are a pair of very intriguing systems due to multiple attributes. Mainly because they are the simplest of polycyclic aromatic hydrocarbons (PAHs) and are isomers of each other. This makes them important targets for understanding fundamental molecular physics. Moreover, az possess very peculiar excited state dynamics which has been of interest for last few decades [1-8]. It is a well-known example of non-conformation to Kasha's rule [9]. Az exhibits much stronger fluorescence out of second electronically excited singlet state, S_2 than the low lying first excited singlet state, S_1 [1]. Ionization potential of az is fairly low, about 7.44 eV, so that a photon tuned to excite S_n (where n>2), will be able to ionize the molecules from any electronic state higher than and including S_2. This in combination with ultrafast internal conversion of az from S_n to S_2 proposes the possibility of production of molecular ion at the ground electronic state with very well defined internal energies [5,7,8]. It is an ideal molecular system to investigate unimolecular photodissociation dynamics as a function of the internal energy in the parent molecular ion.

The interest in these cations is further enhanced by the fact that the family of PAH molecules is expected to explain the conspicuous infrared bands observed from inter stellar medium [ISM] [10]. Amongst many aspects of their molecular dynamics, the interplay of isomerisation and dissociation in PAHs is generally very important in the context of the evolution of PAH population in ISM [11]. There are many groups of isomeric PAHs, most of which have isomerization barriers near or below the dissociation limit. This makes most examples of isomeric pairs difficult to study. The simplest cationic PAH isomers, nph^+ and az^+ are known to undergo isomerisation with an energy difference of 0.8 eV [12]. The transition state barrier energy for isomerization between az^+ and nph^+ is calculated to be about 3.04eV by *ab initio* methods [12]. Whereas the lowest dissociation channels have a barrier height of about 4.5eV [12-14]. Thus dissociation upon isomerisation is possible to explore in the case of the nph^+ and az^+ pair as a function of their internal energies. Probing molecular isomerisation/dissociation using photoemission or photoabsorption is in principle possible, but difficult [11]. Hence it is preferred to have the targeted system in the cationic form and use mass

spectrometry in correlation with time resolved dissociation measurement to search for effects of isomerisation on dissociation. In one of our recent work, isomerisation process of cationic az is identified based on of low energy neutral loss channels [15]. Elimination of atomic hydrogen, molecular hydrogen and acetylene are the low energy dissociation channels of PAH/PAH cations. They are often modelled as Arrhenius type unimolecular decay process governed by the dissociation barrier and internal energy. Therefore, it becomes interesting to vary the internal energy and measure decay rate of specific channel in order to reveal the effects of isomerisation. With a control of the internal energy of the molecule or its cation, a systematic study of isomerisation influenced dissociation process can be undertaken.

One of the possible methods to perform such measurements is to produce cations of PAHs by conventional techniques and then heat them by photo excitation using a tuneable laser. Experimentally, the ionization process itself brings out complications like the determination of residual internal energy after ionisation, formation of multiple conformations of the parent ion etc. Therefore, parent ion is prepared with negligible internal energy before subjecting it to heating process [16, 17]. A single VUV photoionization in combination with photoelectron spectroscopy is a commonly employed technique to investigate the dissociation process of PAH^+ [18]. But it requires access to large synchrotron radiation source facilities and demands prohibitively low event rate to counteract false coincidences. All the methods of highly excited cation production described above finally use an ion storage ring or time of flight (ToF) technique. In the former case, the identity of the decay channel is ambiguous and in later technique the available time window for detectable decay is usually limited to first few micro seconds after cation formation. ToF mass spectrometer combined with an ion trap can target a longer time scales compared to standard linear ToF arrangement, but observations at shorter time scales are disturbed by extraction time uncertainties [14]. In the PAHs, the decay rate of H loss or C_2H_2 loss channels varies in several orders of magnitude for few eVs of shift in internal energy [12,14]. Thus a spectrometer covering a continuous range of time scales from hundreds of nanoseconds (ns) to tens of microsecond (μs) will be most suitable to study isomerisation effects upon dissociation channels.

In this work, a single nanosecond pulsed laser is used to produce PAH cation via a specific ionization mechanism leading to narrow internal energy distribution over a range of wavelength (235-250 nm). A high resolution kinetic energy (KE)-ToF correlated spectrometer is used to achieve the continuous ns-μs timescale in order to observe the effects of isomerization on H loss dissociation channel of az^+. Multi photon ionisation/dissociation is a very well-known and well utilised technique in molecular mass spectrometry. With the powerful approach of time resolved pump-probe spectroscopy, it is often employed to unravel the excited state properties like time scales of fluorescence, internal conversion (IC) and intersystem crossing (ISC), etc. Generally the production of molecular cations using multiphoton interaction is not an appropriate method to obtain narrow internal energy distribution of cations. The broad distribution of internal energyresults mainly by the range of possible photoelectron kinetic energies, rapid radiative decays, etc. The ambiguity is further augmented by non-radiative processes like IC and ISC in the cations. Conventionally two color laser experiments are performed in order to avoid such complications. In which a first color is tuned in such a way that parent ion is produced with negligible internal energy and a second laser heats the molecular ion to a known internal energy. The detailed investigation of excited state dynamics of neutral az has been carried out in past using time resolved pump-probe photoionization technique in association with photoelectron spectroscopy [1-8]. Here we demonstrate that if excited state dynamics of a neutral molecule is known in detail, a single color nanosecond tuneable laser may be sufficient to measure the dependence of internal energy on its dissociation channel.

EXPERIMENTAL SET UP

The details of the instrument used for the present experiment has been described elsewhere [19]. It consists of a time of flight spectrometer combined with a high resolution parallel plate energy analyser (PPA) at the end of drift tube and a nanosecond pulsed laser [Nd:YAG pumped Optical Parameter Oscillator (OPO)]. Briefly, the spectrometer has four critical regions, namely, extraction region (ER), acceleration region (AR), field free drift (FD), and parallel plate analyzer (PPA) region. ER and AR is made up of three parallel plates with each plate having an extraction hole of 0.7mm, all the plates are aligned carefully to match the extraction aperture while keeping the equipotential surfaces parallel. The first plate is biased to +3 kV, followed by +2.35 kV on the second plate and the last plate is at ground potential. This is followed by a long, field free drift region and a large PPA. Neutral vapour azulene at room temperature is allowed to effuse through a small nozzle (with the length to diameter ratio > 50) into the extraction region of the interaction chamber, which is maintained at 5×10^{-8} mbar and is allowed to increase to a maximum of 9×10^{-8} mbar with the gas load. Heating of target sample was not required due to relatively high vapour pressure and high photo absorption cross section of az. A nanosecond pulsed laser which can be tuned for a wide range of wavelength (present experiment is performed between 235-290nm) is focused using a lens of focal length 20 cm near the first plate (2 mm away from the plate), which is at +3 kV. The temporal width of a pulse is approximately 2 ns at a repetition rate of 100 Hz and the average energy of each pulse was 5 μJ corresponding to an intensity of 10^9 W/cm^2. A position sensitive micro channel plate (MCP) detector mounted at the end flange of the ToF tube extended from PPA can detect neutral fragments emitted by drifting parent ion (not used in the present experiment). The ions entering into the energy analyzer are deflected to a parabolic trajectory, with a horizontal range proportional to their KE. As the ion beam complete the parabolic trajectory with a mean range of 500 mm they are detected by a second position sensitive MCP detector (PSD) with delay line anode. This detector in coincidence with laser pulse reference, give the ToF as well as the horizontal position of impact on the detector. The high resolution of the instrument makes sure that even a 0.5% shift in the KE produces a clearly separated feature on the PSD. Schematics of the experimental set up is shown in Fig. 1. In a standard linear ToF spectrometer, an excited molecular ion fragmenting in the extraction or acceleration phase fills the gap between parent and fragment peaks in the ToF spectrum [20]. Hence such fragmentation is investigated by carefully fitting the shape of the feature accompanying the peaks. But a fully accelerated parent ion breaking down in the field free drift (FD) tube would populate the parent ion peak. Therefore the time information of slow fragmentation channels ($\approx k<1x10^6$ s^{-1}) are not available with a conventional ToF spectrometer. This ambiguity can be removed by adding a high resolution energy analyzer at the end of the drift tube as shown on Fig. 1.

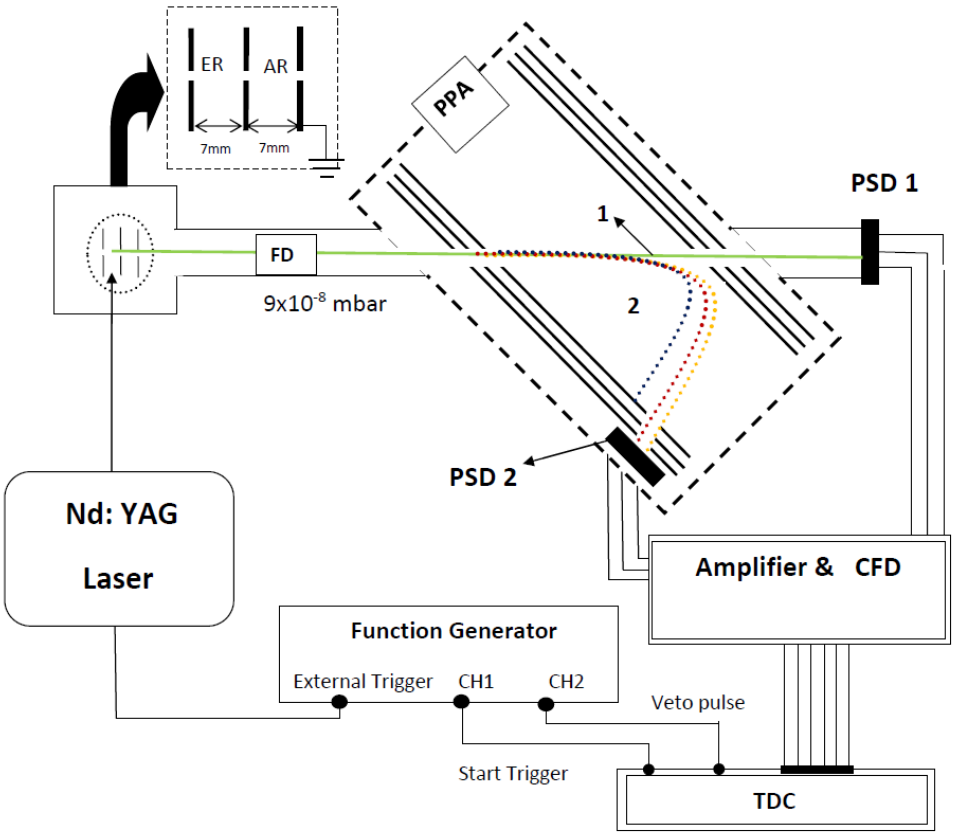

Fig. 1.2D Schematic drawing of the setup showing trajectory of neutral (1) and ion (2) beam as well as data acquisition system.

Laser pulse timing is used as the master trigger as shown in the schematic in Fig. 1. The MCP front signal gives ToF spectra as shown in Fig. 2. The mass resolution is well beyond 1 in 4000 so as to clearly separate various H, H_2 loss as well as isotopic peaks. Note that it is not possible to extract information about H_2 loss compared to sequential H loss using a conventional mass spectrometer. In the present system the KE of fragment ion is also available. Hence a scatter plot of ToF vs KE is very illustrative of differentiating H_2 emission from sequential H loss. To the best of our knowledge this capability is unique in the mass spectrometry of large molecules. Similarly, heavy neutral loss channels like C_2H_2 loss have different ToF distributions as shown in the Fig. 2. This distorted ion peak results from fragment ions produced within the extraction region. Spread in KE of H loss fragment ion produced in ER and AR is within the time width of prompt H loss peak. Therefore, H loss peak has narrow distribution. The decay rate of C_2H_2 loss channel can be estimated by simulating ToF distribution by the exponential decay for the electrical and mechanical configuration of the spectrometer. The information about H_2/2H as well as C_2H_2 loss channel is not included in the present manuscript since the main focus here is to understand role of excited state dynamics in determining the internal energy of the cation produced. In this context it is most suitable to consider an atomic fragment rather than a molecular fragment which might bring up its own complexity. The fraction of parent and fragment yields with respect to total number of laser pulses (1.2% of fragment ions and 5.6% of parent ion)

show that the lower laser intensity restrains the absorption to two to three photons.

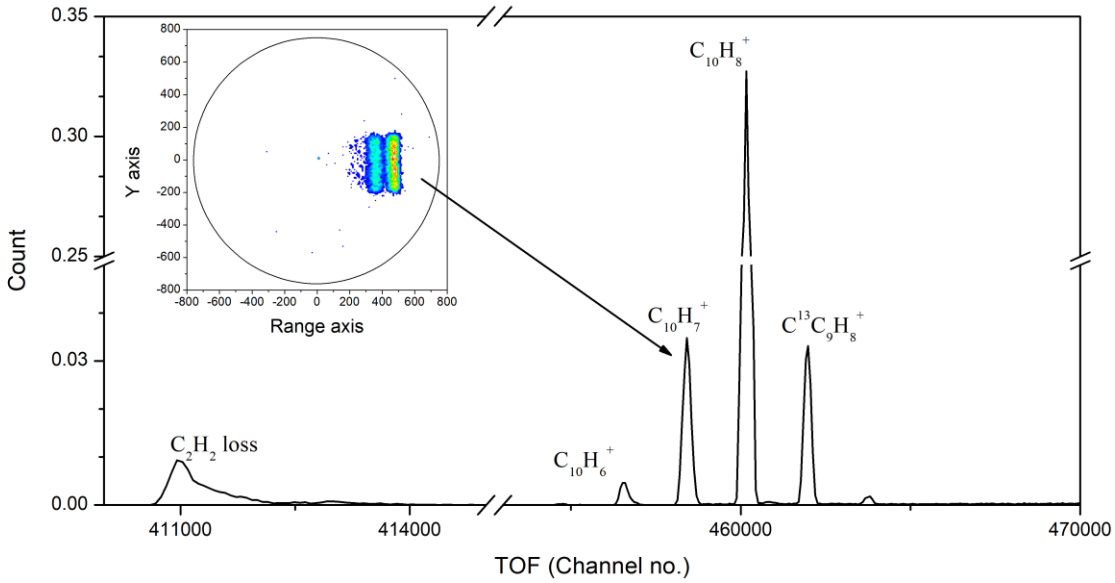

Fig. 2. ToF spectrum of az recorded at 235nm and $9x10^9$ W/cm^2. Inset figure corresponds to the distribution of H loss channel on ion PSD. It separates low and high energy H loss peaks along the horizontal coordinate with a typical resolution of 7eV over 3keV.

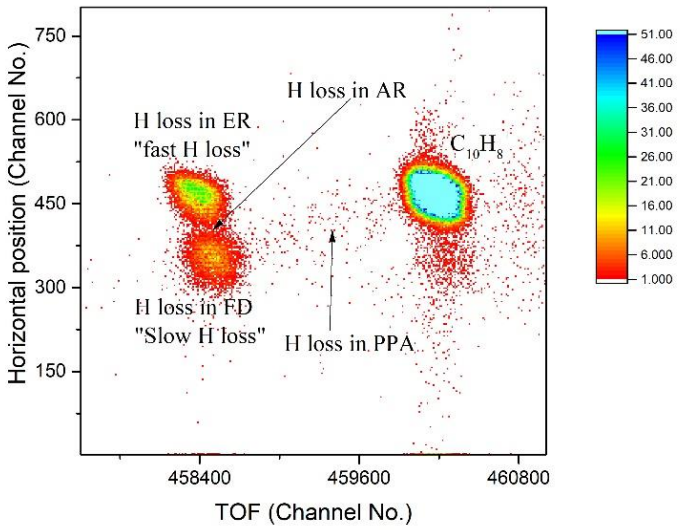

Fig. 3. 2D diagram for ToF vs horizontal position (horizontal position linearly scale to the kinetic energy of the ion) of parent and H loss fragment ion measured at 235nm and $9x10^9$ W/cm^2. Various features in the 2D diagram are marked according to their corresponding decay location.

In the present set up, the intact az^+ spends about 400 ns in the ER and 200 ns in the AR. The FD region is extended about 780 mm length, corresponding to a drift time about 13 μs. A daughter ion produced in the ER or AR will have KE between maximum possible KE (KE of fragment ion produced in the first few nanoseconds after laser pulse) and the fraction of KE proportional to its mass. A fragment ion produced in FD region will have the lowest KE among all the H loss product ions and the KE carried by such fragment ions will be proportional to its mass. Thus, the data obtained with time as well as KE

spread would enable us the prediction of decay time scale. One example of ToF versus KE correlation plot is shown in Fig. 3. Population of H loss fragments is distributed as per their respective decay location. Qualitatively we can identify three possibilities for an internally hot parent ion which is about to lose H. If the H loss occurs in ER or AR region the resulting m/q=127 will be located at the full ToF of m/q=127 (channel no: 458400) and full KE imparted by the extraction and acceleration voltages with channel no: 460 along the y-axis as shown in Fig. 3. This we call as "fast H loss". If the decay occurs in the FD region, the decay population is concentrated about the same ToF as m/q=127 (channel no: 458502) but at ≈0.8% less KE compared to the fast peak (channel no: 350). This island is labelled as "slow H loss" in the 2D graph. If the decay occurs in the PPA region, we will observe a belt connecting full energy parent peak to the slow H loss peak. There is some micro structure to the fast peak and the region connecting fast to slow peak due to the decay dynamics in the ER and AR but considering the small change in KE for single H loss, it is hard to quantitatively analyse this gap between fast and slow peak.

The rate constant information of H loss process can only be extracted from 2D correlation diagram shown in figure 3 with the help of a detailed simulation. Therefore, a probabilistic decay of H loss process is simulated using *Monte Carlo* code for the electric and geometric configuration of the spectrometer. Most important is that the dissociation rate constant is the only adjustable parameter in the simulation which fits the relative population on different peaks appearing in the 2D plot. If the fast H loss peak is only present in the 2D diagram, rate constants must be $k>10^7 s^{-1}$. If H loss population is dominated on the fast and slow peaks, the corresponding decay rates will be between $10^7 s^{-1}$ and $5x10^5 s^{-1}$. The belt corresponding to the decay inside PPA will be populated for decay rates between $5x10^5 s^{-1}$and $10^3 s^{-1}$[See Fig. 6 in Ref. 19]. In our experiment H loss distribution is characterized by both fast and slow H loss peaks with negligible population on the belt for the wavelength range 235nm to 252nm.The ratio of slow to fast H loss yield measured in the experiment is reproduced in the simulation by assigning appropriate decay rate. The ratio between slow and fast H loss yields obtained for each wavelength is discussed in the next section in the context of 3 or 4 photon absorption. The rest of the paper will focus mainly on the slow H loss component of figure 3.

RESULTS AND DISCUSSIONS

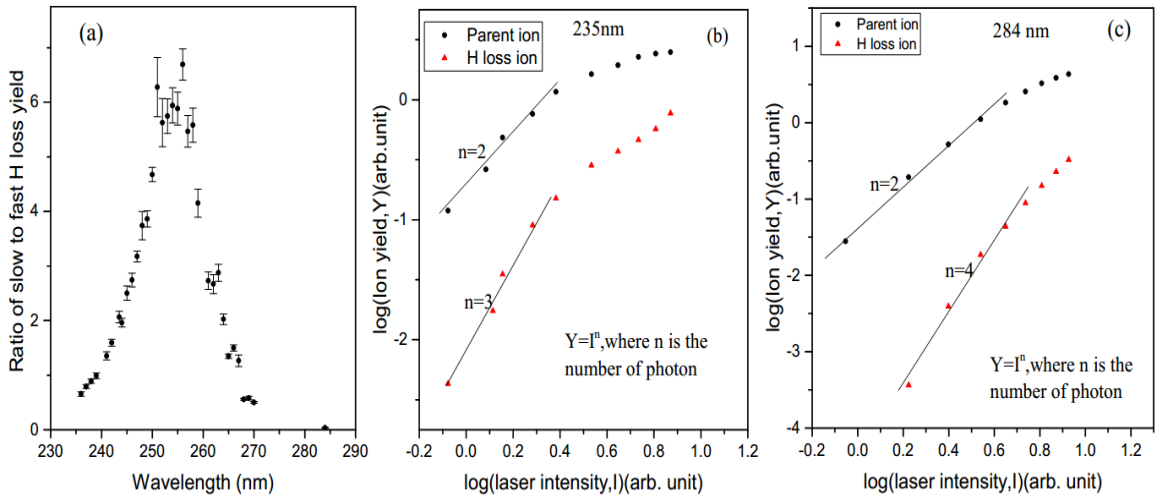

Fig. 4. (a).Ratio of slow to fast H loss yield measured at a range of wavelength 235nm-284nm, Intensity dependence of single ionization of $C_{10}H_8$ and H loss fragmentation yield (both slow and fast contribution) at 235nm (b) and 284nm (c). Solid lines are fits of the $C_{10}H_8^+$ and $C_{10}H_7^+$ data according to indicated power law.

Since both nph as well as az are very well studied systems in terms of their excitation and internal energy dynamics, it is possible to obtain internal energy values for each decay constant. The details of this estimation are evident in the later sections. These internal energy values plus the required ionisation energy at 235 to 250 nm are such that the observed decay rates at these wavelengths is energetically possible via a 3-photon process. Indeed, the apparent energy of H-loss fragment in a single VUV photon ionisation experiment of az is around 14 eV, which corresponds to 3-photon absorption at 265 nm [21]. As we cross 255 nm to longer wavelengths the 3-photon induced decay begins to disappear from the range of observability of the setup. To illustrate this, the ratio of slow to fast H loss yield is plotted in fig. 4(a). The ratio is systematically increasing in the wavelength region 235-255nm as expected from 3-photon absorption with a decreasing internal energy of the cation. The 3-photon process in this wavelength range is separately confirmed by the laser intensity dependence of H loss fragment ion signal as shown in Fig. 4(b). The relative contribution of 4-photon dominated H loss process is negligible at this wavelength region 235-250nm. But after 250 nm the ratio decreases very rapidly indicating increase in the fast H-loss fraction. To explain this wavelength dependency, we invoke a 4-photon absorption process for the decay observed beyond 250 nm. The extra energy added in the 4-photon process (about 4eV) produces a strong fast peak as shown in Fig. 4 (c)at 284nm. The transition from 3 to 4-photon driven H loss yield is shown in Fig. 4(b) & 4(c). From 284nm onwards only fast H loss peak was observed in the mass spectrum as the 3-photon dominated decay was too slow to be observed in the available time window. In conclusion the 2D-plot of figure 3 is assigned by a slow H-loss produced at three photon ionisation and a fast H-loss produced at four photons transition. Let now examine what is the 3-photon ionisation in azulene.

The excitation and ionisation mechanism of az molecule has already been investigated in detail using picosecond (ps) and femtosecond (fs) lasers by pump-probe techniques [5-8]. These experiments have identified electronically excited states of az and characterized their relaxation mechanism by time dependent probe photon ionization. P.M Weber *et al* [5] measured the photoelectron spectra of az obtained upon ionizing the molecule via the S_3 and S_4 states with a transform limited ps pulse. In this work, S_2 ionisation was identified for both the cases from the photoelectron energy spectra. It was demonstrated in those experiments that vibrationally hot molecular ions were produced due to fast internal conversion from S_n to S_2 and subsequent second photon ionization to D_0 while satisfying propensity rule of $\Delta v \approx 0$. V.Blanchet *et al* [7,8] have performed 1+1 photoionization experiments via S_4 states using a fs pulse with wavelength centred at 266 nm and 258nm and identified a significant contribution of the photoelectron signal arising from S_4 to D_1 ionization. In their experiment photoionization takes place on a time scale commensurate with internal conversion. It helped them to set an upper limit (≈120fs) to the lifetime of S_4 and thus timescale of IC.

Thus it is understood from the past results that the IC time scales from the S_n to S_2 states are <100fs. In our experiment, with a ns pulse duration, we can expect that S_n to S_2 relaxation competes very efficiently with a direct ionisation (pathway (a) in Fig.5) and is totally completed before ionisation from a vibrationally excited S_2 state takes place (pathway (b) in Fig.5). Further, S_2 to D_0 ionization satisfies $\Delta v \approx 0$ (pathway (b) in Fig. 5) . Az^+ can be further excited by third photon and can relax back to ground electronic state D_0 by rapid IC [22]. These extremely hot az^+ undergoes IVR and relaxes by various statistical processes as isomerisation and dissociation.

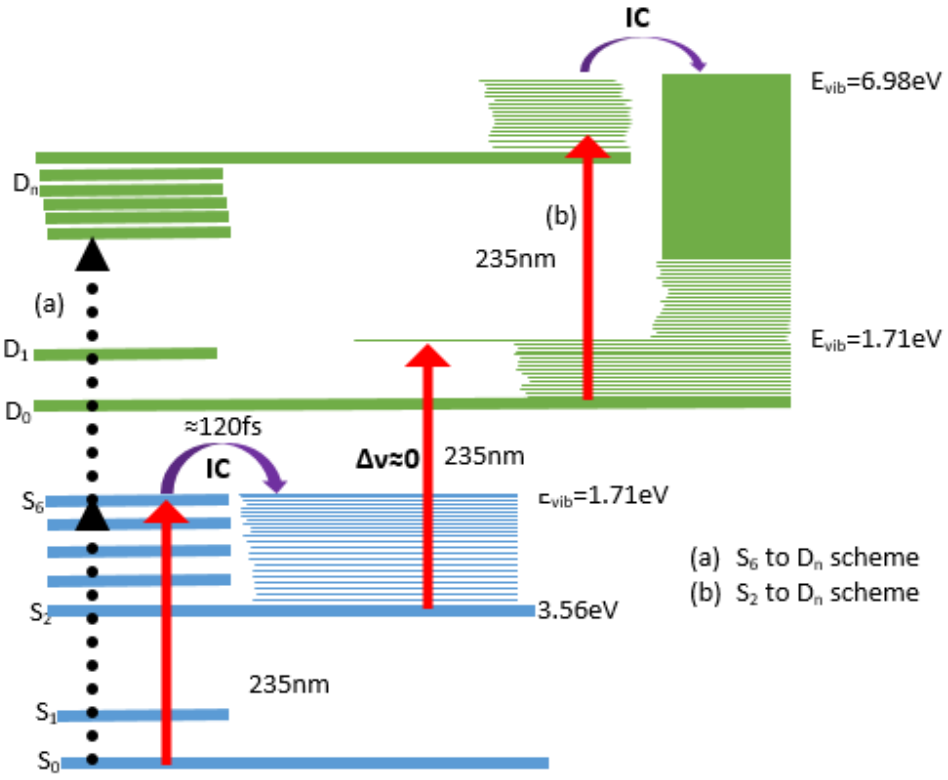

Fig. 5 Schematics of S_2 to D_0 ionization at 235nm in azulene: the dotted black arrows show direct two photon ionsaition (path a) and the three set of continuous red arrows show multipstep 3 photon ionaition-exacitation path (path b)

The dv=0 propensity rule of ionisation, allows to estimate the internal energy of az^+ after the 2nd photon absorption and then after the 3rd photon absorption. This internal energy is in the range of 6.98 to 6.36 eV for 235-250 nm. H loss rate constants of az^+ measured by the present set-up for internal energies proposed by S_2 ionization scheme (pathway b) is given in table.1. It can be compared to the extensive calculations for isomerisation and dissociation rate constants of az^+ for a range of internal energies 5-12.5eV carried out by Dyakov *et al* [12].

Table.1. H loss rate constants measured in the present experiment for internal energies proposed by S_2 ionization scheme (a) is compared with Dyakov's calculation of rate constants (b), (Ref.12) covering the range of internal energies proposed by S_2 ionization scheme.

Present experiment (a)			Dyakov's calculation (b)			
Wavelength (nm)	E_{int} (eV) of az^+	Diss. Constant of slow H loss (s^{-1})	E_{int} (eV) of az^+	Direct H loss rate (s^{-1})	Isomer. rate (s^{-1})	Reverse isomer. rate (s^{-1})
235	6.98	$1.5x10^6$	7.99	$2.0x10^5$	$8.7x10^7$	$1.3x10^7$
250	6.36	$3.3x10^5$	6.42	$2.8x10^2$	$2.8x10^6$	$2.3x10^5$

As per Dyakov's calculation it is clear that az^+ to nph^+ isomerisation is the dominant process for the expected internal energies. The most recent computations and experiments show that the transition barrier of isomerization of az^+ to nph^+ lies below the low energy dissociation limits of az ion [12, 13]. W. Cui et al [16] have performed time resolved photo dissociation experiment for az^+ and nph^+ ion and observed that the acetylene loss channel (which is another low energy parallel dissociation channel) of these isomeric ion is measured to have similar decay rates at a deficit of internal energy about 0.8eV for az^+ (In this experiment $E_{int}(az^+)$=6.2eV and E_{int} (nph^+)=7eV). This is explained on the basis of fast conversion of az^+ to the lowest energy isomer nph^+ prior to dissociation at the relevant internal energies. In a couple of experiments and high level computations isomerization energy of az^+ to nph^+ is independently predicted to be about 0.8eV [12, 23]. As per Dyakov's rate calculations [Ref 12, Table.3], isomerisation of cationic azulene is at least two orders of magnitude faster than its direct H loss for the internal energies expected from our 3-photon absorption scheme [See table.1]. In conclusion, for our experimental timescales (about 10μs) isomerization is dominating so that it produces nph cation at elevated internal energies by about 0.8eV compared to Az+. Therefore, it can safely be assumed that whatever H loss process observed for the first 10μs is mainly coming from nph^+ isomer. Hence hereafter we consider dissociation curve of cationic nph for further discussions.

A. Comparison of internal energy with S_2 ionization scheme

Gotkis *et al* [14] have modelled time resolved break down curve for H loss fragment ion of nph using rate-energy constants obtained via RRKM/QET calculations for a range of internal energies 4-12eV. H loss dissociation curve of nph^+ proposed by Gotkis *et al* is studied along with other advanced calculations carried out by Dyakov *et al* and Solano and Mayor [12,14,24]. The present experiment only measures rate constants of slow H loss decay at 235-250nm. The rate-energy calculation carried out for nph^+ by Dyakov *et al*. were used to convert this information into corresponding internal energy with the help of necessary interpolation. Dissociation rate k(E) and corresponding internal energy (E_{int}) identified from previous calculations is listed in table.2. As discussed before, we extend S_2 to D_0 ionization scheme as suggested by P.M Weber *et al* [5] to all the measured wavelengths as shown below to predict the internal energy of az^+ after successive absorption of 3-photons.

$E_{S2 \rightarrow D0}(az^+)$=[E(photon) - S_2(v=0) (3.56eV)]+E(photon), Δv≈0 is allowed……(1)

Where S_2 is the second electronic excited state energy. Therefore internal energy of isomerized ion, nph^+ will be

$E_{S2 \rightarrow D0}(nph^+) = E_{S2 \rightarrow D0}(az^+) + E_{iso}$ (0.8eV)……..(2), where E_{iso} is the isomerisation energy

Table.2. Dissociation rate constants measured in the present experiment are listed along with the corresponding internal energy, E_{int} identified from the H loss dissociation curve of nph^+ [14]. Internal energy predicted as per S_2 to D_0 ionization scheme is shown separately.

Wavelength for az (nm)	Dissociation rate experimentally measured k(E), (s^{-1})	Estimated Internal energy (E_{int}) of nph^+, (eV), [Ref.12]	Estimated Internal energy via $E_{S2\rightarrow D0}$ (nph^+) (eV)
235.0	$1.50x10^6$	7.97	7.80
236.0	$1.46x10^6$	7.96	7.74
237.0	$1.45x10^6$	7.96	7.70
238.0	$1.20x10^6$	7.89	7.66
239.0	$1.00x10^6$	7.82	7.62
240.0	$9.00x10^5$	7.78	7.58
241.0	$8.80x10^5$	7.78	7.52
242.0	$8.00x10^5$	7.74	7.48
243.0	$6.50x10^5$	7.67	7.44
243.5	$6.50x10^5$	7.66	7.42
245.0	$5.60x10^5$	7.61	7.36
246.0	$5.00x10^5$	7.58	7.32
248.0	$4.00x10^5$	7.50	7.24
250.0	$3.30x10^5$	7.43	7.16

E_{int} identified in the experiment by comparing the measured rate constants with the calculations done by Dyakov [12] is compared with the value predicted by S_2 to D_0 ionization schemes for 235-252nm as shown in Fig. 6. The average internal energy deduced from the present experiment is in qualitative agreement with the S_2 to D_0 ionization scheme for 235-252nm though the estimates are systematically higher by about 0.25 eV compared to the values predicted by the S_2 to D_0 ionisation model.

Experimentally deduced E_{int} curve lies above E_{int} curves modelled via S_2 to D_0 ionization scheme consistently. At this juncture a few possible reasons can be proposed for such higher internal energies. It is possible that various vibrational levels in the S_2 manifold are involved in the ionization scheme, moreover higher the vibrational energy in the S_2 state, more difficult is to fulfill $\Delta v \approx 0$ transition. Hence other energetically allowed ionization transitions can gain significant intensity through a vibronic coupling between nearby electronic states. Similar ionization via S_1 band is observed for nph [25]. It may also be noted that for wavelength shorter than 250 nm D_1 ionisation also become energetically feasible. Though the $\Delta v \approx 0$ transition between S_2 and D_1 have never been experimentally observed, it is still offered as a possible contributing mechanism here, only on the basis of energetics. If such propensity is assumed for S_2 to D_1 transition then the resulting internal energy will be consistently higher by about 1.1 eV and cause much faster decay. Estimates of E_{int} under these assumption are plotted in Fig. 6 for reference. Finally, it may be noted that the experiment was done using az vapour at room temperature, thus considering the total degrees of freedom, about 0.3 eV internal energy is already known to be there in the molecular gas.

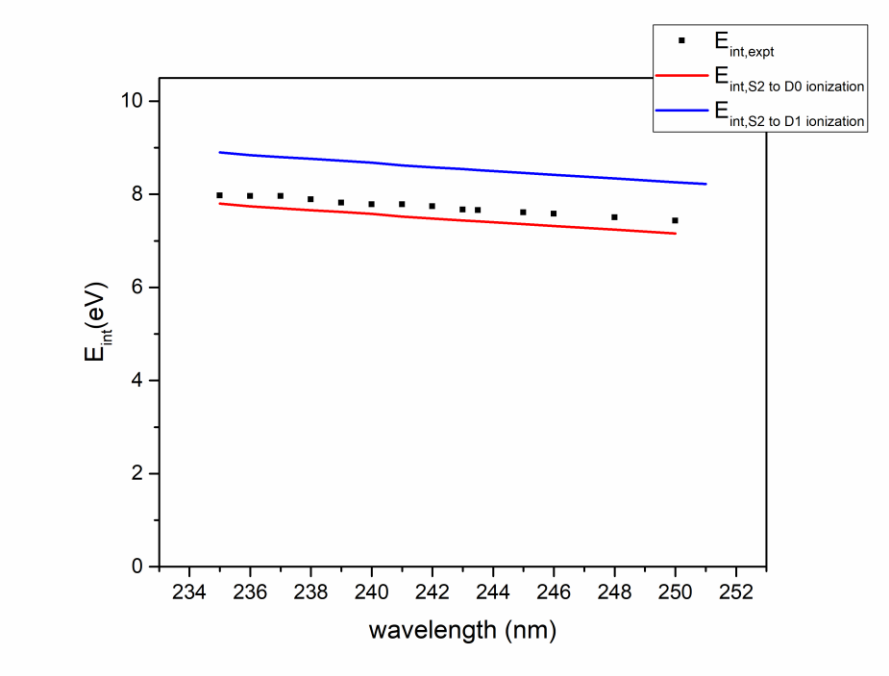

Fig. 6. Internal energy in Naph+ deduced from the experiment (black squares) for 235-252nm and predicted via S_2 to D_0(red line) and S_2 to D_1 (blue line) ionization of Az+ is plotted. S_2 ionization schemes serve as limits to the internal energies.

CONCLUSION:

A unimolecular dissociation process of neutral H loss from az^+ is discussed here in the light of its peculiar excited state dynamics, a part of which is common to all PAHs. An additional dimension of kinetic energy measurement to conventional ToF mass spectrum has helped us extract decay constants of unimolecular dissociation of az^+ over a long time scale. As single nanosecond tunable pulsed laser was used to accomplish this complex task which otherwise requires much more complex combination of ionisation and excitation mechanisms. A single nanosecond high intensity laser pulse in general can cause a severe ambiguity in the internal energy after a multi photon ionisation process. A careful study based on the excited state properties of neutral az and a systematic comparison with H loss dissociation process of its low energy isomer nph^+ , has helped us to ascertain the excitation as well as 2-photon ionisation mechanism induced by ns pulsed UV excitation. Moreover, we have demonstrated that prediction of the internal energy of dissociating ion is possible in this context. And hence a systematic internal energy dependence on H loss mechanism of az^+ was made possible. The chosen photon energy in conjunction with the observable timescale of the 2D-instrument made sure that direct loss of H from az cation would not interfere in the measurement. We obtained a consistent result over a broad range of wavelength considering an ultrafast population transfer from S_n states to S_2 before ionisation by a second photon absorption. The internal energy of the cation thus formed is boosted by third photon absorption. This gives rise to a very hot cation of az with a well defined internal energy, which is then shown to undergo rapid isomerization to nph^+ over a range of wavelength 235-250nm. It is a known exothermal process. This heats the new nph cation further and shifts the H loss dissociation kinetics to the visible time-range of the spectrometer.

Thus in this work we are able to demonstrate that by the virtue of rapid IC process and vibrational propensity rule due to the structural rigidity of PAHs can be exploited to produce narrow internal energy distributions of PAH cations. Apart from its value for the molecular dynamics of PAHs, this

process will be very useful as an experimental technique in multitudes of PAHs investigations. Particularly those which involve ion traps or ion storage rings. This peculiar one-color ionisation scheme is now being extended to multiple PAHs with considerable success.

- AUTHOR INFORMATION

Corresponding author at: Indian Institute of Space Science and Technology, Thiruvananthapuram 695547, Kerala, India.

*E-mail: umeshk@iist.ac.in. (Dr. Umesh R Kadhane)

REFERENCES

[1] M. Fujii, T. Ebata, N. Mikami, M. Ito, Chem. Phys. 77 (1983) 191.

[2] J. R. Cable, A. C. Albrecht, J. Chem. Phys. 84 (1986) 1969.

[3] L. Ciano, P. Foggi, P. R. Salvi, J. Photochem. Photobiol. B 105 (1997) 129.

[4] M. Damm, F. Deckert, H. Hippler, J. Troe, J. Phys. Chem. 95 (1991) 2005.

[5] P. M. Weber, N. Thantu, Chem. Phys. Lett. 197 (1992) 556.

[6] N. Kuthirummal, P. M. Weber, Chem. Phys. Lett. 378 (2003) 647.

[7] V. Blanchet, K. Raffael, G. Turri, B. Chatel, B. Girard, I. A. Garcia, I. Wilkinson, B. J. Whitaker, J. Chem. Phys. 128 (2008) 164318.

[8] P. Piecuch, J. A. Hansen, D. Staedter, S. Faure, V. Blanchet, J. Chem. Phys. 138 (2013) 201102.

[9] M. Kasha, Discuss. Faraday Soc. 9 (1950) 14.

[10] A. G. M. M. Tielens, Annu. Rev. Astron. Astrophys. 46 (2008) 289.

[11] A. J. Haas, J. Oomensab, J. Bouwman, Phys. Chem.Chem. Phys. 19 (2017) 2974.

[12] Y. A. Dyakov, C. K. Ni, S. H. Lin, Y. T. Lee, A. M. Mebel, Phys. Chem.Chem. Phys. 8 (2006) 1404.

[13] G. Koster, C. Lifshitz, J. M. L. Martin, J. Chem. Soc., PerkinTrans.2 11 (1999) 2383.

[14] Y. Gotkis, M. Oleinikova, M. Naor, C. Lifshitz, J. Phys. Chem. 97 (1993) 12282.

[15] M. V. Vinitha, P. K. Najeeb, A. Kala, P. Bhatt, C. P. Safvan, S. Vig, U. R. Kadhane, J. Chem. Phys. 149(19) (2018) 194303.

[16] W. Cui, B. Hadas, B. Cao, C. Lifshitz, J. Phys. Chem. A 104 (2000) 6339.

[17] N. Van-Oanh, P. Désesquelles, P. Bréchignac, J. Phys. Chem. A 110 (2006) 5599.

[18] B. West, C. Joblin, V. Blanchet, A. Bodi, B. Sztaray, P. M. Mayer, J. Phys. Chem. A, 116 (2012) 10999.

[19] M. V. Vinitha, A. Kala, S. Kumar, U. R. Kadhane, Rev. Sci. Instrum. 90 (2019) 103304.

[20] H. Kühlewind, A. Kiermeier, H. J. Neusser, J. Chem. Phys. 85 (1986) 4427.

[21] H. W. Jochims, E. Ruhl, H. Baumgartel, S. Tobita, S. Leach, Int. J. MassSpectrom. Ion Processes 35 (1997) 167.

[22] S. Hirata, M. H. Gordon, J. Szczepanski, M. Vala, J. Phys. Chem. A 107 (2003) 4940.

[23] H. W. Jochims, H. Rasekh, E. Ru¨hl, H. Baumga¨rtel, S. Leach, Chem. Phys. 168 (1992) 159.

[24] E. A. Solano, P. M. Mayer, J. Chem. Phys. 143 (2015) 104305.

[25] C. R. Martin Cockett, H. Ozeki, K. Okuyama, K. Kimura, J. Chem. Phys. 98 (1993) 7763.